

# TEST STATION FOR REED SENSORS AND INDUCTIVE PROXIMITY SWITCHES

Viktória ÁCS<sup>1</sup>, János TÓTH<sup>2</sup>

<sup>1</sup> University of Debrecen, [acsviktorias6@gmail.com](mailto:acsviktorias6@gmail.com)

<sup>2</sup> University of Debrecen, [tothjanos@eng.unideb.hu](mailto:tothjanos@eng.unideb.hu)

**Abstract**—The aim of our work was to design and implement a programmed system combined with movement. Our system can visualize, record the signals of the connected sensor with proper sampling speed and displays it for evaluation. The test station is capable of carrying out a sampling speed to detect the typical characteristics of the Reed sensor. The created measuring system is therefore capable of filtering the uncertainly operating sensors, and can be used for the examination of the seemingly faulty sensors as well.

**Keywords**— characteristics, inductive, LabVIEW, myDAQ, National Instruments, Reed, sensor

## I. INTRODUCTION

THE aim of our work was to design and implement a system combined with movement. Our system can record the signals of the sensor with proper sampling speed and displays it for evaluation. During our work, Reed sensors and inductive proximity switches were used.

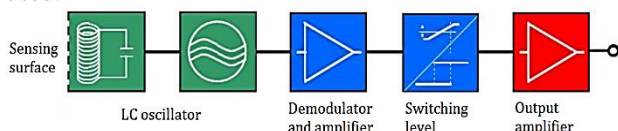


Fig. 1. The inductive proximity switch, P. Bánlaki and A. Lovas [1]

The inductive proximity switches detect metal objects without contact, and are characterized by a long service life and extreme ruggedness. If there is a conductor object nearby, the generated magnetic field creates eddy currents in the metal and the switch operates according to P. Bánlaki and A. Lovas [1].

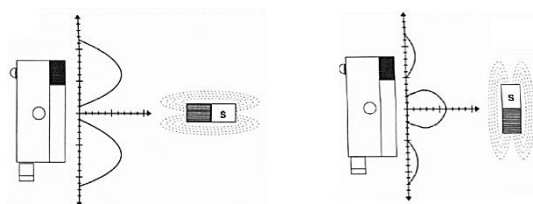


Fig. 2. The characteristics of the Reed sensors, P. Bánlaki, A. Lovas [1] and Gy. Krámlí [2]

The Reed sensor is an electrical switch operated by an applied magnetic field. Fig. 1. shows that the sensor provides several switching ranges which depend on the position of the magnet by P. Bánlaki, A. Lovas [1] and Gy. Krámlí [2].

The magnetic induction is a vector quantity which represents the strength of the magnetic field.

In a linear coil the magnetic field is considered homogeneous, which depends on the number of threads (N), the coil length (l) and the current density (I) and, where ' $\mu_0$ ' is the vacuum permeability.

$$\mathbf{B} = \frac{\mu_0 \cdot \mathbf{I} \cdot \mathbf{N}}{l} \quad (1)$$

The magnetic field also depends on the ' $\mu_r$ ' relative permeability factor, which gives an increase in the value of the magnetic field when using a variety of different than air cores.

$$\mathbf{B} = \frac{\mu_0 \cdot \mu_r \cdot \mathbf{I} \cdot \mathbf{N}}{l} \quad (2)$$

The magnetic field strength:

$$\mathbf{H} = \frac{\mathbf{B}}{\mu} \left[ \frac{\text{A}}{\text{m}} \right] \quad (3)$$

$$\mu = \mu_0 \cdot \mu_r \quad (4)$$

where ' $\mu_r \approx 1$ ' in case of para and diamagnetic materials, while in case of ' $\mu_r \gg 1$ ' ferromagnetic materials.

Furthermore, when a ferromagnetic material is used the following relation is observed:

$$\mathbf{B} \neq \mu \cdot \mathbf{H} \quad (5)$$

$$\mathbf{B} \approx \mu \cdot \mathbf{H} \quad (6)$$

The characteristic of induction-field strength of the ferromagnetic materials (iron, nickel, cobalt and their alloys) is strongly non-linear, the determination is made

by measurement. Fig. 3. shows the magnetization curve, and the first magnetization can be observed thereon, where  $H_m$  is the maximum field strength,  $H_c$  is the coercive field strength, while  $B_r$  is the value of the remanent induction.

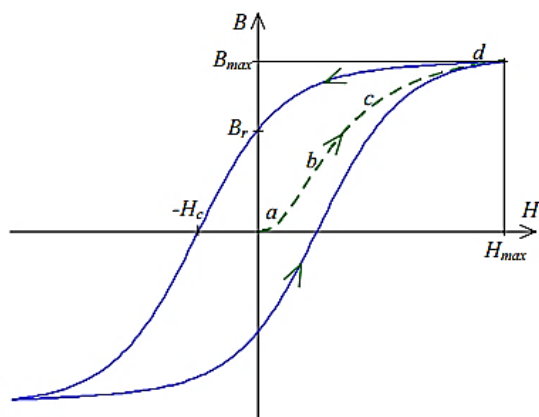


Fig. 3. The magnetization curve, I. Kádár [3]

Neodymium disc magnets (VMM9-N48) with nickel surface protection were used during our studies.

Rare earth elements such as neodymium have ferromagnetic properties. Neodymium alloy magnets ( $Nd_2Fe_{14}B$ ) are the strongest permanent magnets known. Table I. shows the main properties of the magnets by A. Verma, O. P. Pandey and P. Sharma [4].

TABLE I  
 PROPERTIES OF THE MAGNETS

Magnet type	Remanence ( $B_r$ ) [mT]	Coercivity ( $H_{cb}$ ) [kA/m]	Maximum total energy ( $BH_{max}$ ) [ $kJ/m^3$ ]
neodymium ( $Nd_2Fe_{14}B$ )	1200-1300	800-1200	210-250
ferrite (MF25)	350-400	240-320	27.5-31.5

## II. THE OPERATION OF THE TEST STATION

During the project, we had to create a system that includes the data acquisition device, the sensors, electronics and mechanics and a computer which runs the evaluating program and also controls the devices.

In the following the constructed system is demonstrated and the resulting relationship between main parts are described.

The constructed system consists of an NI myDAQ (National Instruments Data Acquisition Device) ('A'), a moving system ('B'), a motor control circuit ('C'), voltage adaptation ('D'), the sensor ('E'), power supply ('F') and a computer ('G').

A 24 VDC power supply is supplying to the sensor and the motor through the motor control circuit. The signal and the ground wire was connected to the voltage adaptation, which creates 10 VDC voltage, so it can be safely connected to the NI myDAQ device input ports,

since it can endure  $\pm 10$  VDC, S. Újvári, A. Magyarkuti [5].

The data acquisition device is responsible for the operation of motor control circuit, which actuate the movement system. When the limit switches of the moving system are switch, they send a signal to the myDAQ device that completely stop the system or starts the motor the other way, depending on how much was the number of displacements.

A FESTO SME-8-K-LED-24 sensor is an electric proximity switch with internal Reed sensor, which has a working voltage 12-30 VDC and NO (Normally Open) contact.

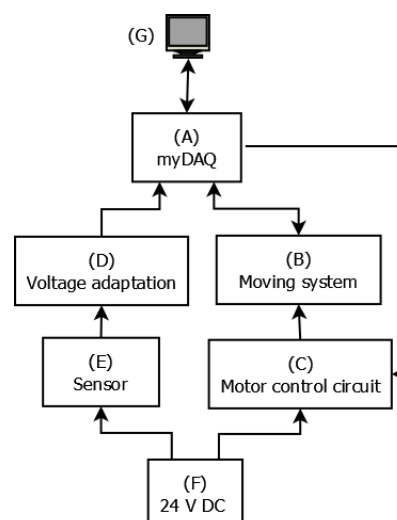


Fig. 4. The schematic structure of the system

As an inductive proximity switch Baumer IFRM 06P1503/S35L was used, that also has normally open and has 12-30 VDC working voltage.

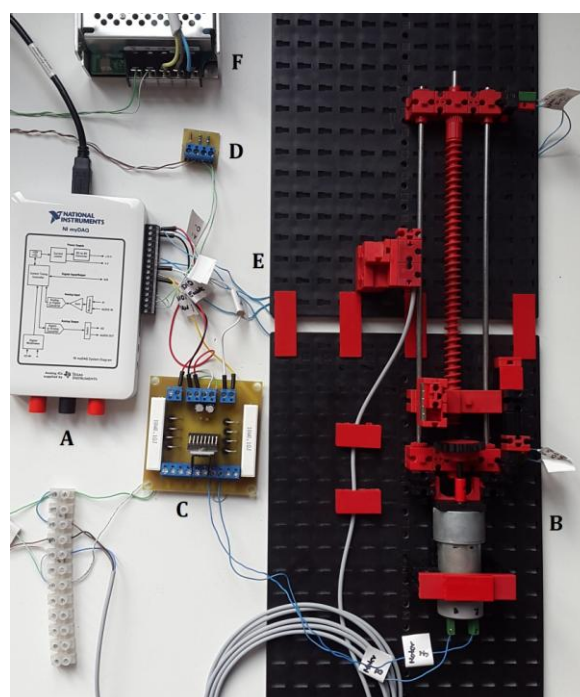


Fig. 5. The built system

### A. NI myDAQ

In the built system, the National Instruments myDAQ device is signed with 'A' in the previous figures. It can be seen that the data acquisition device is connected directly or indirectly to all of the main parts.

The data acquisition ('A') is in direct contact with the computer, on which the program is responsible for the detection, the movement and the evaluation. It is in direct connection with the motor control unit ('C'), since the conditions defined in the program sends a signal to move to one or the other direction, and sends a signal to the device through the program in case of a limit. Furthermore, it connects via the voltage adaptation circuit ('D') to the sensor ('E'), since it cannot be connected directly because of the input voltage ( $\pm 10$  VDC) of the myDAQ analog input ports.

### B. Sensor moving system

Since for Reed sensors the magnet is worth applied in two different position (parallel to the sensor, the north pole is in line with the moving direction and then perpendicular, when the north pole pointing towards the sensor), so we had to create a frame that is easily changed, R. H. Bishop [6].

Morse-type 'fischertechnik' limit switches were used. The myDAQ +5 VDC was connected to the '1' connector and the normally open connector ('3') was attached the myDAQ digital input (DIO Digital Input or Output) port (positive limit switch 'DIO4', negative limit switch 'DIO3'). When the system reaches an end position, the contact is closed, so the +5 VDC signal is sent to the myDAQ. Sensing this input will stop further movement, then reversed move in direction or stop the process depending on the number of repetitions the system have performed.

### C. Motor control

The direction of 24 VDC motor rotation can be changed when the polarity of the voltage is changed, therefore we made a circuit including an H-bridge integrated circuit (L298N IC). The circuit is designed for controlling two DC motors which can be switched on or off with a dedicated input (Enable A, B) independently.

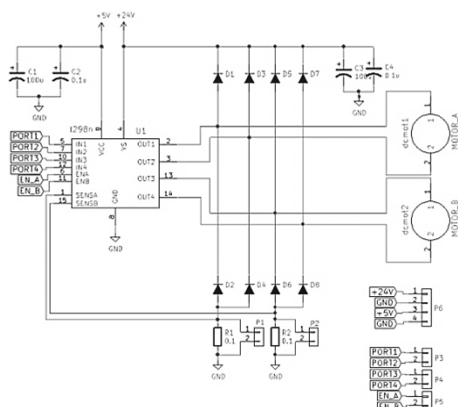


Fig. 6. Motor control circuit

As shown in Fig. 6, we used two kinds of power supply in the designed circuit. The +5 VDC power comes from the myDAQ device, which is responsible for operating the gate circuits, while the +24 VDC power supplies the external power supply, it is responsible for operating the motor.

Since originally the circuit is capable of simultaneously driving two DC motors, but we were only need one, so we did not use up all provided inputs and outputs. To 'Out1', 'Out2' we connected the motor, while 'Out3' and to 'Out4' outlets were not connected during this project.

The mentioned Enable ('EN\_A', 'EN\_B'), enable input corresponds with two independent H-bridges. The 'EN\_A' outlet was connected to the myDAQ 'DIO0' (Digital Input or Output) port.

We do not use all the connections on the input side as well. The 'IN1' and 'IN2' input are responsible for driving the 'A' motor one or the other direction, while 'IN3' and 'IN4' are for the 'B' motor. If 'IN1' receives input signal from myDAQ 'DIO1' port then motor starts in one direction, provided that the EN\_A also receives a signal. Under the same conditions when 'IN2' input from 'DIO2' port, it will rotate in the opposite direction.

### III. MEASUREMENT PROGRAM

The program was made with LabVIEW v2013. Laboratory Virtual Instrument Engineering Workbench (LabVIEW) is a development environment from National Instruments.

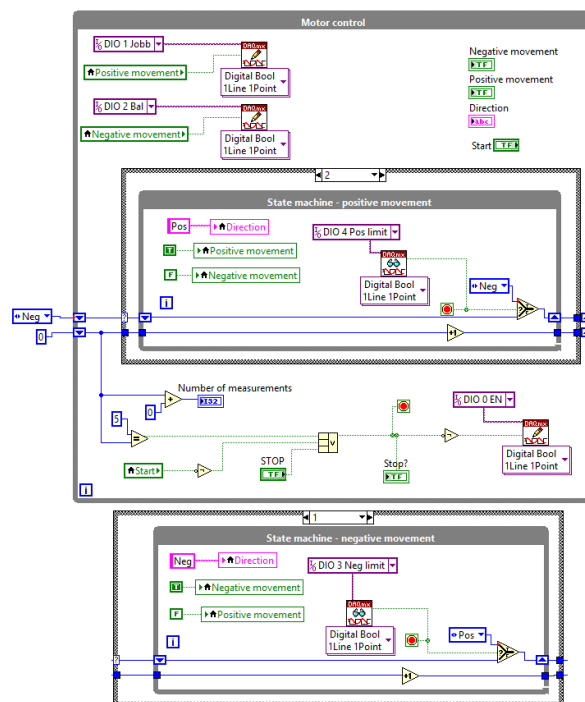


Fig. 7. The total motor control program

During the development of the program the first major part was the motor control unit. The segment, which is

responsible for moving the system can be seen in Fig. 7. Since the motor control circuit input Enable ('DIO0') I had to give a signal continuously, but 'IN1' ('DIO1') and 'IN2' ('DIO2') ports are alternately needed, therefore, we solved with one of the commonly used design pattern, with a state machine that includes a variety of conditions [7], [8]. However, the system can be in only one state at a time, and transitions between them are strictly defined.

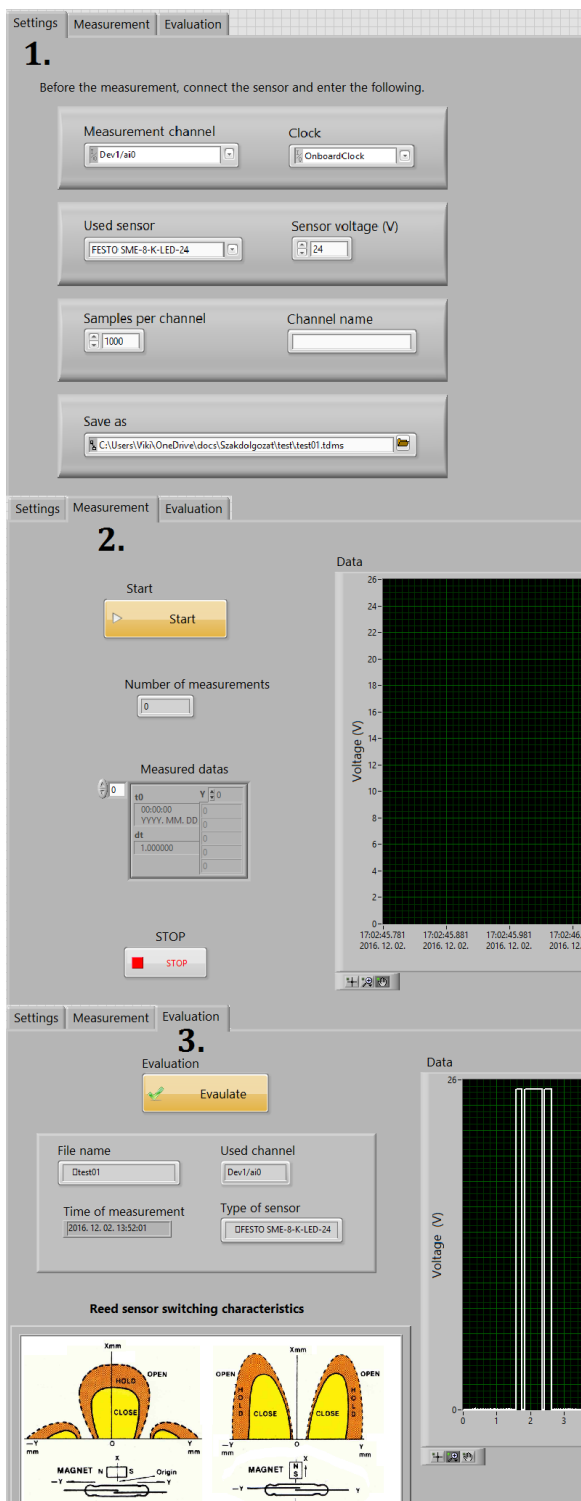


Fig. 8. The Front Panel

The program consists of three main parts and in the Front Panel the user can switch between them. The first is the 'Settings' (1.) where the entering of options for the measurement can be carried out.

The next window (2.) is intended to carry out the implementation of the movement and the measurement. The graph continuously displays the current values during the measurement.

The evaluation can be found in the last section (3.). The settings that were specified in the first panel are read back to the program, and it displays them in the required information (File name, used channel, sensor type, measurement time) and includes a graph that displays the complete series of measurement values in an easily understandable way.

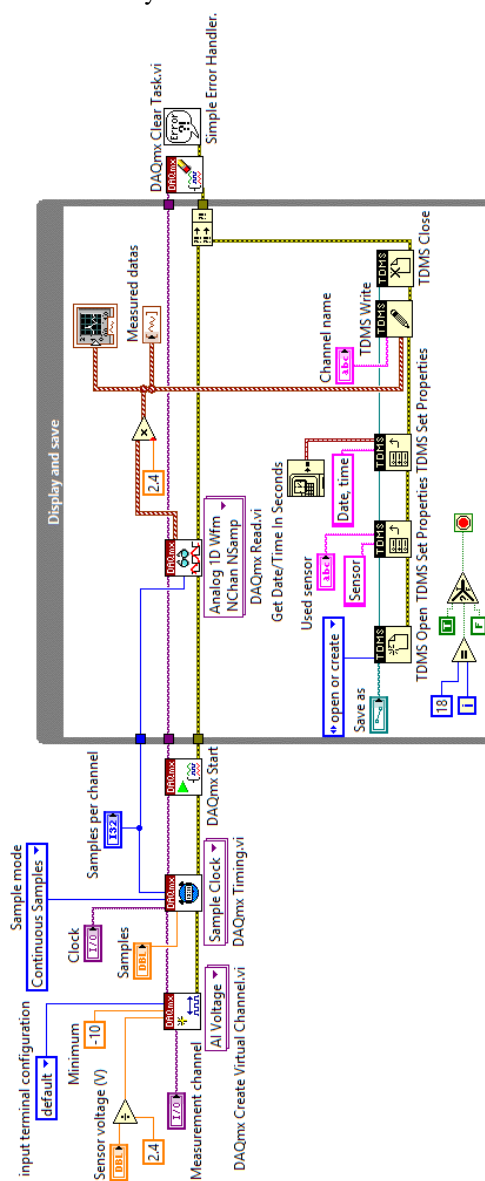


Fig. 9. The measuring program

The program segment that is responsible for measuring voltage was created an analog input (AI) channel using the DAQmx Create Virtual Channel.vi (virtual instrument). This required a controller which is displayed

on the Front Panel ('Measurement Channel'), where the physical measurement channels can be selected and also the sensor power supply can be adjusted, which will be reduced by the ratio of the voltage adaptation. Using the DAQmx Timing.vi was using we set the clock used during the measurement, the sampling frequency and the number of samples per channel, and then set the DAQmx Start Task.vi to run.

The continuous measurement happens within the While loop on the based on the previous settings, display, and export the data to a \*.tdms file (TDMS - Technical Data Management Streaming). Outside the loop there is the DAQmx Clear Task.vi to stop and cancel the job opened, thereby releasing the resources that are used in the activity.

#### IV. EVALUATION

The third component in Front Panel is in charge of evaluating all of the measured data. In case of an active state of 'Evaluate' switch, the software will open the saved file using the 'TDMS Open' from the saved location control with the use of a local variables. Then the program reads the data and the used channel in the measurement with 'TDMS Read', and the collected properties of the logged file using the 'TDMS Get Properties' block. The first three elements of the 'cluster' contain the name of the file that was created, the sensor type and exact measurement time.

The evaluation process does not actually require myDAQ device connected to it, because you only need to file \*.tdms to create the graph. Henceforth we would like to illustrate and analyse graphs obtained during the evaluation.

The measurements were carried out several times in parallel and perpendicular position relative to the sensor to be satisfied that there is no measurement error.

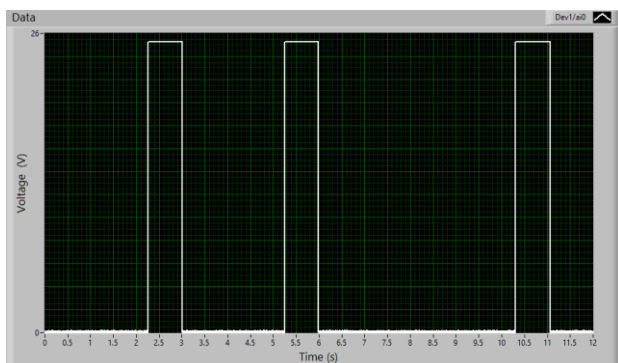


Fig. 10. Characteristic of IFRM 06P1503 sensor in parallel position

Fig. 10. shows the switching characteristics we measured when the Baumer IFRM 06P1503/ S35L type was used. In the first case, the magnet is positioned parallel to the detection surface, and then the magnet is rotated 90°. In this case, the image shown in Fig. 11. was obtained. The two diagrams in fact only differ from each

other, that in first situation the longer side of the magnet was facing the sensing surface, while in the second shorter side, so it remained within sensing range for a shorter time as well.

The real challenge was to measure the characteristics of the Reed sensors, because as stated earlier, was shown in Fig. 2., approaching the sensor laterally it may result two or even three switching on and off ranges in certain configurations.

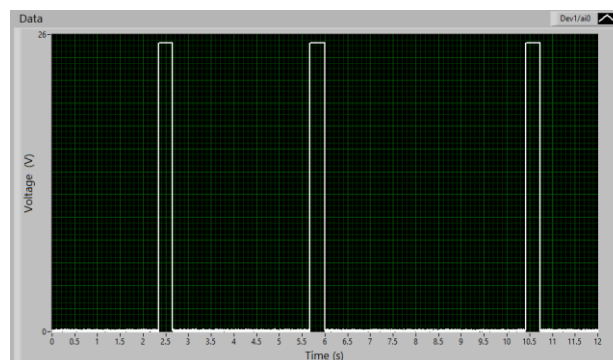


Fig. 11. IFRM 06P1503 characteristic in perpendicular position

The used sensor was a FESTO SME-8-K-LED-24, which was placed parallel to the magnet first. After multiple measurements, we were able to detect the characteristics seen in Fig. 12. with the tools we used. It can be observed the typical nature of the Reed sensors triple segmented characteristic, which is a result because of the three times on and off switching.

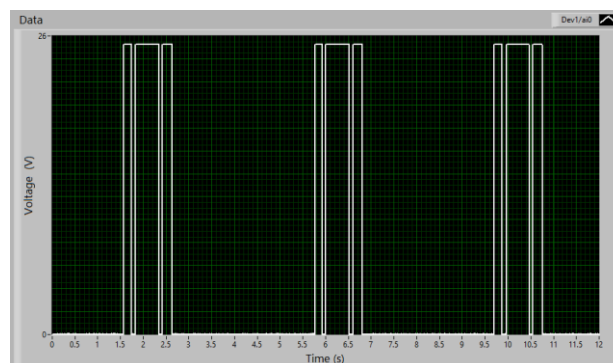


Fig. 12. SME-8-K sensor characteristic in parallel position

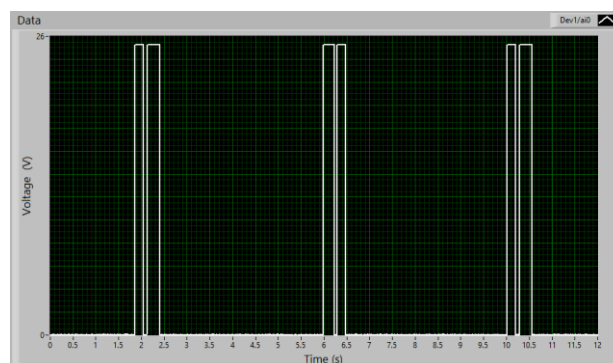


Fig. 13. SME-8-K sensor characteristic in perpendicular position

In case of perpendicular magnet position the FESTO SME-8 sensor shows the curve seen on Fig. 13. This supports the nominal characteristics of the Reed sensors, shown in Fig. 2. based on the professional literature data.

The newly created measuring system is therefore capable of filtering the uncertain operating sensors, and can be used for the examination of the seemingly faulty sensors as well.

#### V. SUMMARY

We came to the conclusion on the basis of the measurements that the program we created and the equipment used is capable of carrying out a sampling speed to detect the typical characteristics of the Reed sensor.

We managed to build a small and compact sized device. The front panel of the program is user-friendly, clear and it is easy to navigate. As a result, we are able to measure in the thousandths of a second with the tools used and to view and analyse detail-oriented.

The developed system can become more accurate, more efficient and easier to use with a few improvements. We plan on designing more precise, more accurate sensor and magnet holder that would eliminate the measurement errors due to accidental movements.

These fasteners could be made with 3D printing, which is compatible with the existing mounting grooves.

In the future, we want to develop a more complex

processing system, which does not leave user evaluation of the charts to the users, but it automatically and displays.

Although a conclusion may review the main points of the paper, do not replicate the abstract as the conclusion. A conclusion might elaborate on the importance of the work or suggest applications and extensions.

#### REFERENCES

- [1] P. Bánlaki, A. Lovas, "Materials of sensors" (Szenzorika és anyagai), Budapest: Typotex Kiadó, 2012, p 48-56.
- [2] Gy. Krámlí, "FESTO Sensors" (FESTO Szenzorika) FESTO Kft., Budapest, 2007, pp 3-22.
- [3] I. Kádár, "Alternating current systems" (Váltakozó áramú rendszerek), [https://vet.bme.hu/sites/default/files/tantargyi\\_fajlok/h,%202015/04/13%20-%2009%3A40/magnes\\_2.pdf](https://vet.bme.hu/sites/default/files/tantargyi_fajlok/h,%202015/04/13%20-%2009%3A40/magnes_2.pdf), accessed on January 2017.
- [4] A. Verma, O. P. Pandey and P. Sharma, "Stroncium ferrite permanent magnet – An overview" *Indian Journal of Engineering & Material Sciences*, vol. 7, Dec. 2000, pp. 364-369 <http://nopr.niscair.res.in/bitstream/123456789/24430/1/IJEMS%207%285-6%29%20364-369.pdf>
- [5] S. Újvári, A. Magyarkuti, NI myDAQ user manual and specifications (NI myDAQ használati utasítás és specifikáció), [http://sukjaro.eu/ELFT-NI-palyazat/myDAQ\\_magyar.pdf](http://sukjaro.eu/ELFT-NI-palyazat/myDAQ_magyar.pdf), accessed on November 2016.
- [6] R. H. Bishop, *The Mechatronics Handbook*, Boca Raton FL: CRC Press, 2002.
- [7] *LabVIEW Core 1 Participant Guide Course Software Version 2014*, Austin, Texas: National Instruments Corporation, 2014.
- [8] *LabVIEW Core 2 Participant Guide Course Software Version 2014*, Austin, Texas: National Instruments Corporation, 2014.